Comparative Study of the CO_2 Methanation Activity of Hydrotalcite-Based Nickel Catalysts Generated by Using Different Reduction Protocols

Alexandra Müller[1] · Pit Völs[1] · Bianca Störr[1] · Florian Mertens[1]

Abstract

Parameters controlling the reduction of nickel hydrotalcite-based catalysts have been investigated in order to optimize the activity of the catalyst for CO_2 methanation. Beside the variation of temperature and duration in the reduction process of the catalysts with hydrogen, two different reduction modes have been explored. The first one is the direct reduction of the dried uncalcined hydrotalcite-based precursor material whereas the second one is given by the reduction of the same type of precursor material but having been subjected to a calcination step prior to reduction. The corresponding kinetic measurements for the two principally different catalyst preparation schemes reveal that omitting the calcination step can largely be beneficial. Standard characterization data (XRD, BET, TG-FTIR, XPS) for the different catalytic materials will be presented.

Graphical abstract
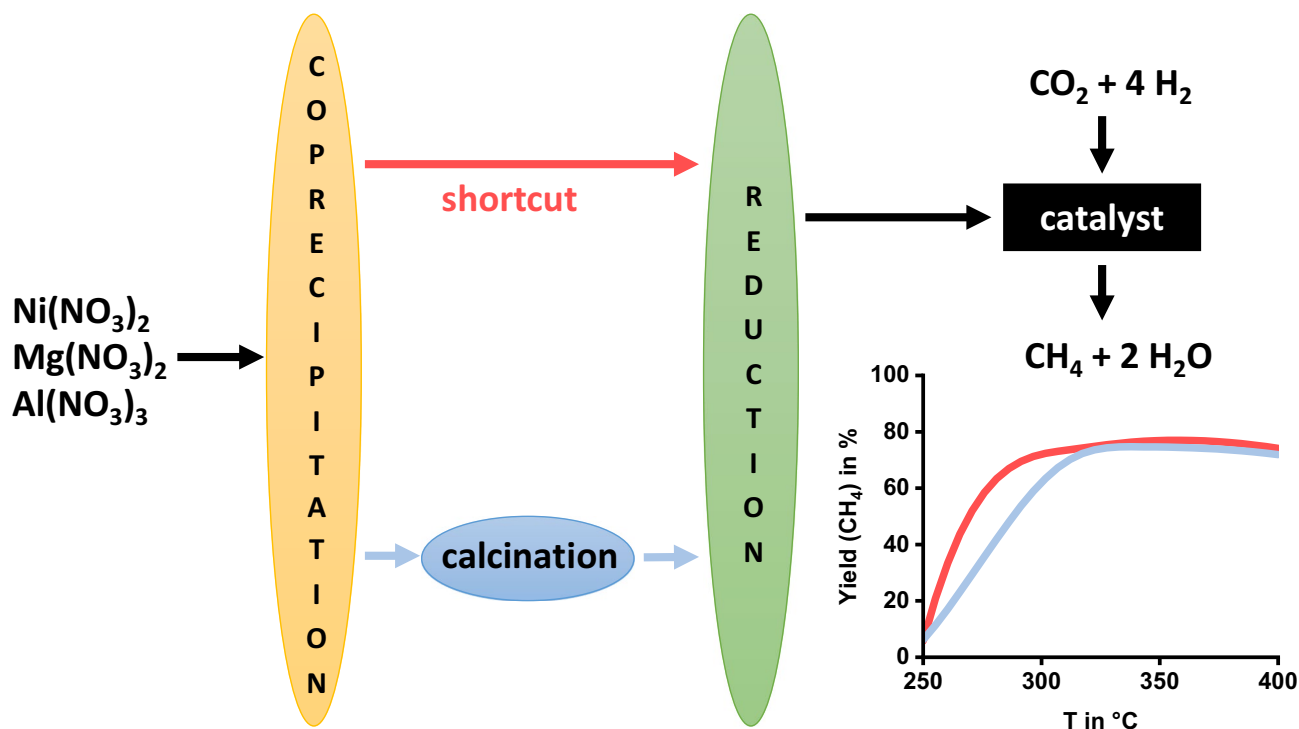
Extended author information available on the last page of the article

1 Introduction

Global warming is to be counteracted and therefore CO_2 emissions are to be reduced [1]. As a consequence, many strategies have been developed among which the storage and utilization of CO_2, i.e. its storage in caverns and its conversion to chemicals, which can be used as green fuels, are currently very actively explored [2].

Due to the intended shift from fossil to renewable energies, large scale energy storage is a requirement to compensate the volatility in energy delivery from renewable sources. Omitting the cost of energy conversion and comparing only the cost of storage, there is a cost benefit if the energy storage is volume based such as for fuels in tanks, pipes, and other containers compared to storage relying on 2-d structure such as battery electrodes.

One approach that combines the diminution of CO_2 emission and the use of renewable energies is the power-to-gas concept, which is to be mainly carried out as power-to-hydrogen or power-to-methane [3]. Storing energy by converting otherwise emitted CO_2 to methane bears the advantage that this product can easily be fed into the natural gas grid, which allows to utilize an already existing infrastructure for large scale energy storage [3].

Various catalysts can be used to hydrogenate CO_2 to methane. Because of the availability and the price, nickel catalysts are preferentially used [4]. These catalysts usually display high selectivity towards methane, but are not resistant to oxidation [4]. Most of the relevant nickel based catalysts are supported and modified by promoters [5].

Since CO_2 methanation is thermodynamically favored at low temperatures, high catalytic activity at the lowest possible temperatures is of particular industrial interest [5] and the search for better catalysts sometimes only exploiting small differences in synthesis still continues [6].

In co-precipitation procedures, in which the metals are simultaneously precipitated as metal salts by a basic solution [7], the conversion to elemental metal and/or metal oxides is needed to obtain the catalytically active species. This conversion is a fundamental step that determines the morphology of the final catalyst and thus its activity [8]. The resulting morphology is also determined by a subtle interplay of the calcination and reduction steps. This is even more so since the calcination itself may influence the necessary reduction conditions [9], which increases the complexity of the optimization problem. With higher calcining temperatures, higher reduction temperatures may be needed for a similar degree of reduction [10]. However, to avoid problems with sintering, the reductions should be carried out at the lowest possible temperatures [11].

In respect to catalytic activity, hydrotalcites are very versatile catalyst precursor materials which allow to be modified by simultaneously incorporation of different metal ions into their structure that may become part of the final catalyst potentially improving the active material, the support or acting as promotors [12–17]. Support materials may be changed to increase surface area and thus the number of catalytically active centers that are accessible. Given these beneficial properties, nickel containing hydrotalcites promise to have large potential for the improvement of CO_2 methanation catalyst although, so far, comparably few studies have been carried out in this regard [6, 16, 18–22].

In order to get enhanced adsorption of the acidic gas CO_2 in this type of catalyst, basic oxides can be used as promotors or even as supports [16, 23]. Hydrotalcites are mixed hydroxides of divalent and trivalent ions, which are built up in layers [12, 13, 24, 25]. By incorporation magnesium into this structure, a catalyst can be prepared that will contain magnesium oxide as a basic component to bind CO_2 more strongly [2, 26]. Regarding this option, hydrotalcites appear to be particularly suitable for precursor materials for the development of CO_2 methanation catalysts applicable at reaction temperatures below 300 °C [6, 26]. A high metal dispersion in these materials leads the formation of Ni nanoparticles with a narrow size distribution enabling good activities to be achieved even with low metal loadings and contributes to the improved performance surpassing the ones of impregnated catalysts [6, 16, 27–29].

2 Experimental

2.1 Catalyst Preparation

A hydrotalcite-based catalyst consisting of 20 mol% nickel, 30 mol% aluminum and 50 mol% magnesium was synthesized by co-precipitation according to the protocol by Mette et al. [7]. For this purpose, a 0.4 mol/L aqueous solution of nickel nitrate, aluminum nitrate and magnesium nitrate was used. An aqueous solution of 0.9 molar sodium carbonate/ 0.6 molar sodium hydroxide was used as precipitation agent. The precipitation was carried out at 50 °C, at pH 8.6 under constant stirring. After the precipitation, the product was aged for half an hour. The solid was filtered off and the precipitate was washed with distilled water until the electric conductivity of the filtrate was less than 500 µS/cm. The precipitate was then dried at 110 °C for 8 h in air.

The dried sample was divided into two batches for two different series of tests. In the first series, the dried catalysts were calcined at 600 °C for 8 h and then reduced at the respective conditions. In the second series of experiments, the dried catalysts were reduced directly.

All the following experiments were carried out with particles ranging in size from 150 to 250 µm in diameter.

2.2 Reductions

The respective reductions for XRD and BET measurements were carried out by heating to 500, 700 or 900 °C with a heating ramp of 5 K/min followed by either one, 4 or 8 h holding time. A gas mixture of 5 vol% H_2 in 95 vol% Ar applied with a total volume flow of 100 mL/min was used to perform the reduction. The prepared reduced catalysts were handled inertly at all times to ensure equal conditions for further investigations.

For the catalytic investigations, the catalysts were reduced directly in the catalytic test stand for 1 or 4 h with the reduction parameters set to the same values as given above.

2.3 XRD

The XRD measurements were carried out using a D2 PHASER diffractometer from Bruker AXS with Cu–K$_\alpha$ radiation.

The analysis was performed in the 2Θ range from 5 to 80° with a counting period of 1 s and a step size of 0.05° 2Θ.

To reduce the risk of oxidation, the reduced catalysts were placed at the sample holder under inert conditions and covered with a foil to protect the sample during the measurement.

2.4 BET

The measurements of the specific surface areas were carried out by nitrogen cryoadsorption using the BELSORP-mini II (BEL JAPAN, INC.) apparatus. Prior to the measurements, the samples were dried in vacuum at 80 °C for 12 h (dried precursor) or at 150 °C for 3 h (calcined precursor and reduced catalyst). Table 1 lists the mean values from two measurements each.

2.5 Catalytic Measurements

The catalytic investigations were carried out in a fixed bed reactor at atmospheric pressure. For this purpose, a glass reactor filled with about 40 mg of the previously calcined or about 50 mg of the dried catalyst was used. The reduction was then carried out directly in the reactor under the reduction conditions given above.

The reaction gas mixture used for the subsequent catalytic tests consisted of 48 mol% H_2, 12 mol% CO_2, 35 mol% N_2 and 5 mol% Ar. The WHSV was set to 3500 mL/g$_{Kat}$h based on the mass of the non-reduced catalyst used. The activity of the catalyst was examined in the temperature range from 250 to 400 °C in temperature steps of 30 K.

Table 1 BET results of the different catalyst materials

Sample	BET surface in m²/g	
	Directly reduced	Previously calcined
Dried	103	
Calcined		152
Reduced 500 °C 8 h	254	226
Reduced 700 °C 1 h	252	218
Reduced 700 °C 4 h	235	215
Reduced 700 °C 8 h	210	
Reduced 900 °C 1 h	159	174
Reduced 900 °C 4 h	166	144
Reduced 900 °C 8 h	101	

The composition of products and reactants was analyzed online by GC (Agilent 7890 A).

2.6 TG-FTIR

The reduction process was tracked by TG-FTIR measurements. For this purpose, the dried and calcined samples were heated at a rate of 5 K/min up to 800 °C in a stream of argon gas containing 10 vol% H_2. IR spectra of the emitted gaseous products were recorded.

2.7 XPS

XPS measurements were carried out in a spectrometer from Specs equipped with the Phoibos 150 analyser. The reduced samples were prepared and transferred into ultrahigh vacuum under inert conditions to avoid re-oxidation. For excitation, a monochromatic XR50 x-ray tube equipped with an aluminium anode (1486.74 eV) was used. The spectra were measured with a pass energy of 15 eV. The charging of the nonconducting samples was compensated using a flood gun. Fitting procedures for data evaluation were carried out with the CasaXPS software. For energy calibration, the Mg2p signal at 49.5 eV [30] of magnesium oxide was used.

3 Results and Discussion

3.1 XRD and BET

Given that the presented investigation is intended to address differences in the catalytic performance of hydrotalcite derived catalysts and that these differences will be strongly connected to the structural and morphological differences resulting from the type of preparation, the investigation of the structural changes by powder XRD between
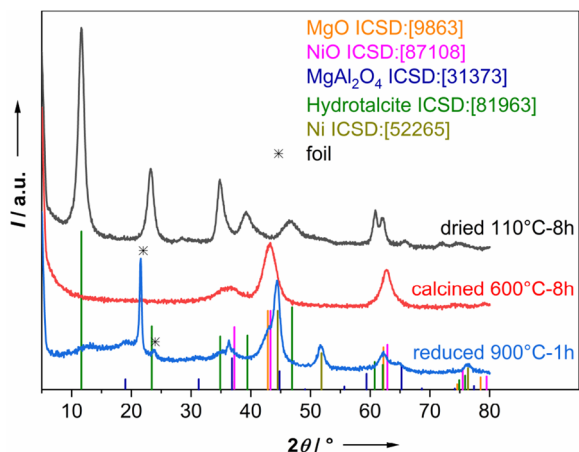
Fig. 1 XRD measurements of dried, calcined and directly reduced catalyst precursor material listed with the applied conditions. Conditions labels are given as temperature-duration pairs (e.g. 110 °C—8 h dried at 110 °C for 8 h). Diffraction patterns based on the ICSD-database entries of reference materials are also shown

Fig. 2 XRD measurements of directly reduced catalyst precursor material listed with the applied reduction conditions. Reduction condition labels are given as temperature-duration pairs (e.g. 700 °C—4 h reduction at 700 °C for 4 h). Diffraction patterns based on the ICSD-database entries of reference materials are also shown

the various stages of catalyst preparation is essential. As can be seen in Fig. 1, the hydrotalcite structure of the dried precursor changes during calcination and reduction to an oxidic matrix with metallic nickel. In Fig. 1, the dried precursor (black line) displays the powder XRD pattern of the hydrotalcite-like structure which can be seen by comparing it to the reference pattern (in dark green). During calcination, the observed structural change is accompanied by the loss of interlaminar water and the emission of carbon dioxide from the hydrotalcite resulting in the formation of an oxide matrix which contains nickel oxide, magnesium oxide, and amorphous Al_2O_3. The applied reduction procedure leads to the conversion of nickel oxide to metallic nickel. Additionally, diffraction peaks indicating the formation of spinels are also seen in the XRD pattern.

Diffractograms of directly reduced samples subjected to different reductions protocols are shown in Fig. 2. Significant differences resulting from the parameter variation in these protocols can be seen in the final structural composition of the obtained catalysts. If the reduction temperature is above 700 °C, the corresponding XRD patterns show reflections from metallic nickel. At 500 °C there are essentially no signs of metallic nickel observable in the diffractogram even after a duration of 8 h for the reduction process. Here, either very amorphous or no metallic nickel at all is formed. The reduction at 900 °C results in remarkably narrower signals than at 700 °C, as well as in the presence of additional reflections indicating the formation of spinels (e.g. $MgAl_2O_4$ or $NiAl_2O_4$). Since the spinels are difficult to reduce to obtain metallic nickel particles, their formation defines the upper temperature limit for an effective reduction procedure, which is therefore, as
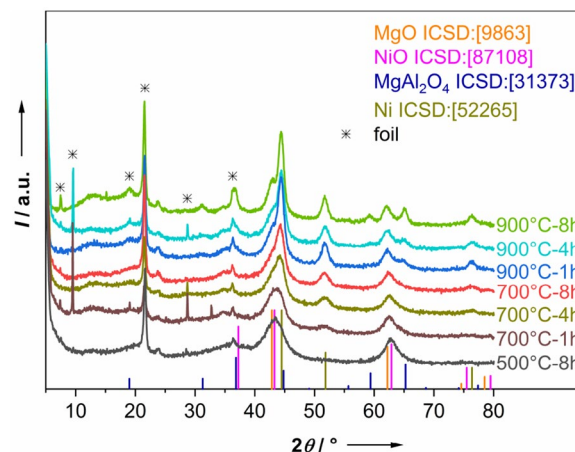
a whole, limited to temperatures above 500 °C and below 900 °C [31].

Figure 3 displays the diffraction patterns of the reduced samples that were previously calcined. They show nearly the same dependency on the reduction conditions as the directly reduced samples with the particularly important fact that for a reduction temperature of 500 °C no signal of reduced nickel is observed. Starting from a reduction temperature of 700 °C reflections of reduced nickel become visibly. These
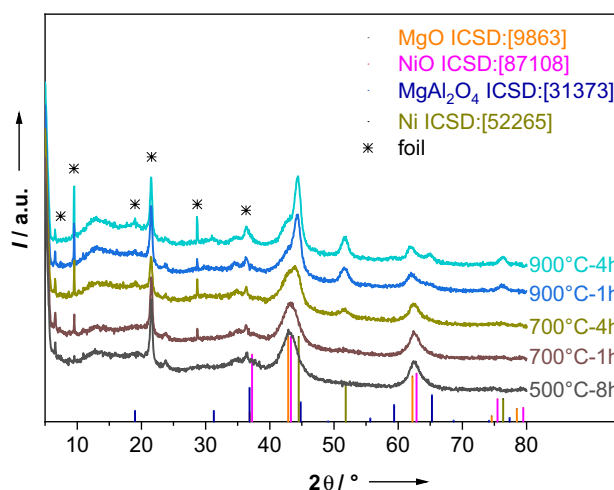

Fig. 3 XRD measurements of previously calcined reduced catalyst precursor material listed with the applied reduction conditions. Reduction condition labels are given as temperature-duration pairs (e.g. 700 °C—4 h reduction at 700 °C for 4 h). Diffraction patterns based on the ICSD-database entries of reference materials are also shown

signals also get narrower with increasing reduction temperature and duration. For a reduction temperature of 900 °C there are signals of a spinel formed. Hence in the diffractograms, there is no particular difference whether or not the samples are calcined prior to reduction.

The investigation of the BET surface area values of the reduced samples display a strong dependence on temperature and duration that can simply be interpreted by assuming that the obtained values are largely influenced by mass transport effects and/or sintering, i.e. high temperatures and long duration allows crystallites to grow and to agglomerate and thus to reduce the BET surface area values. As shown in Table 1, the largest surface area was measured at the lowest reduction temperature (500 °C). The higher the reduction temperature, the lower are the obtained specific surfaces area values. If the specific surface area is compared for reductions at the same temperature, but with differences in the reduction duration, the specific surface area is found to be mainly larger for shorter reduction times, except for the 900 °C experiments of directly reduced samples, where a slight increase was even observed for the increase of the reduction period from 1 to 4 h. The difference is small enough, however, that the values can be regarded as being essentially the same assuming some experimental error. This observation does not mean, that all transformation processes have come to an end as can be seen from the drastic change in surface area to 101 m^2/g for an 8 h reduction period. The direct reduction at 700 °C for 1 h results in a surface area similar to that if the reduction is performed at 500 °C for 8 h.

The previously calcined samples show smaller surface area values for nearly all reduction conditions than the directly reduced samples. Only for a reduction at 900 °C for 1 h, the surface area of the directly reduced sample is smaller than for the previously calcined one and is thus again the only outlier that does not follow the general trend. Altogether, the preceding calcination of the samples is disadvantageous for the surface area of the reduced catalysts.

3.2 Catalytic Measurements

The mass loss by water and CO$_2$ of the precursors during the preparation process differs and therefore the amount of active material per mass of the catalyst varies too. This aspect has to be kept in mind if catalyst activities are compared. There are different experimental conditions between the measurements of directly reduced and previously calcined catalysts, which also have to be taken into account when making a comparison. Two series of experiments have been performed. For the first series of experiments, dried precursor was directly reduced. In this case there is mass loss during the reduction process due to continued drying and interlaminar water loss, calcination processes, and the actual reduction. In the second series

of experiments calcined precursor material was reduced. Here, the observed mass loss can fully be attributed to the actual reduction reaction.

Since the exact mass loss is not known, the WHSV for the catalytic studies was in both cases determined based on the initial material mass taken prior to reduction. Accordingly, the samples belonging to the first series contain a smaller amount of active material than the samples from the second one. To be exact, both series of measurements are therefore not directly comparable. At the same time, both sets reach similarly high activities in the high temperature region but strongly differ in the low temperature one. Given that the sample of the best performing catalyst of the first series generated by direct reduction performs much better than the catalyst samples of the ones produced with a separate calcination step and contains a smaller amount of active material, it is legitimate to conclude that the corresponding catalyst itself is more active and that a quantitative comparison gives at least a lower bound for specifying this improvement.

In the case of the directly reduced samples, apart from one sample (reduced at 700 °C for 4 h), all catalysts display roughly the expected yield and CO$_2$ conversion curves known from the literature [3] (see Fig. 4, top and middle). The catalysts, which have been reduced at 700 and 900 °C, already display a conversion rate of 70% at 310 °C and a constant yield from about 340 °C onward. The samples reduced at 500 °C show low activity over a wide temperature range, while the samples reduced at 700 and 900 °C achieve very high methane yields. A comparison of the catalytic activities of the samples reduced at the same temperature, either at 500 or 900 °C, but for different periods of time shows that the yields at these conditions differ very little. In contrast to that, samples which have been reduced at 700 °C for 4 h display a very different behavior compared to samples reduced at the same temperature but only for a much shorter period of time (1 h). Conducting the reduction directly with the given gas mixture at 700 °C for 4 h results in the highest yield at the lowest temperature of all of the directly reduced samples that we have investigated. For these catalysts, a yield of methane of 80% at 250 °C, which then increases with higher reaction temperature only slightly, was found.

The selectivities of the directly reduced samples are shown in Fig. 4 bottom. It can be seen that the selectivities of the samples reduced at 700 and 900 °C are nearly the same and close to 100% over the whole temperature range. If the catalysts are reduced at 500 °C, a selectivity of about 100% is also seen in the region of highest yield but at temperatures below 280 °C, where the catalyst is not very active, the resulting selectivity is also low. Selectivities over 100% originate from small errors in the calibration curves of the gas chromatograph. These errors have a larger impact when the conversion rate is low due to mathematical issues.
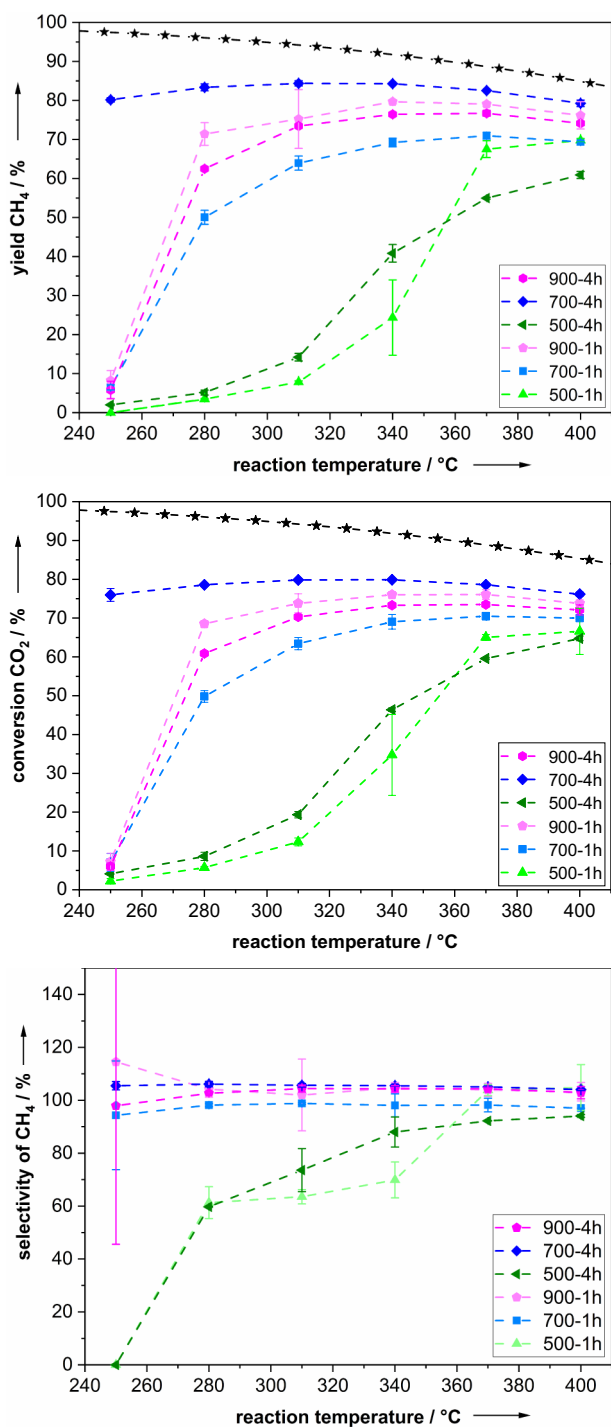
Fig. 4 Top: methane yield of catalysts from precursor directly reduced at different conditions: green triangle—reduction at 500 °C, blue square—reduction at 700 °C, pink circle—reduction at 900 °C and reduced for different periods of time; black stars—thermodynamic equilibrium. Middle: CO₂ conversion, Bottom: selectivities corresponding to the measurements in top
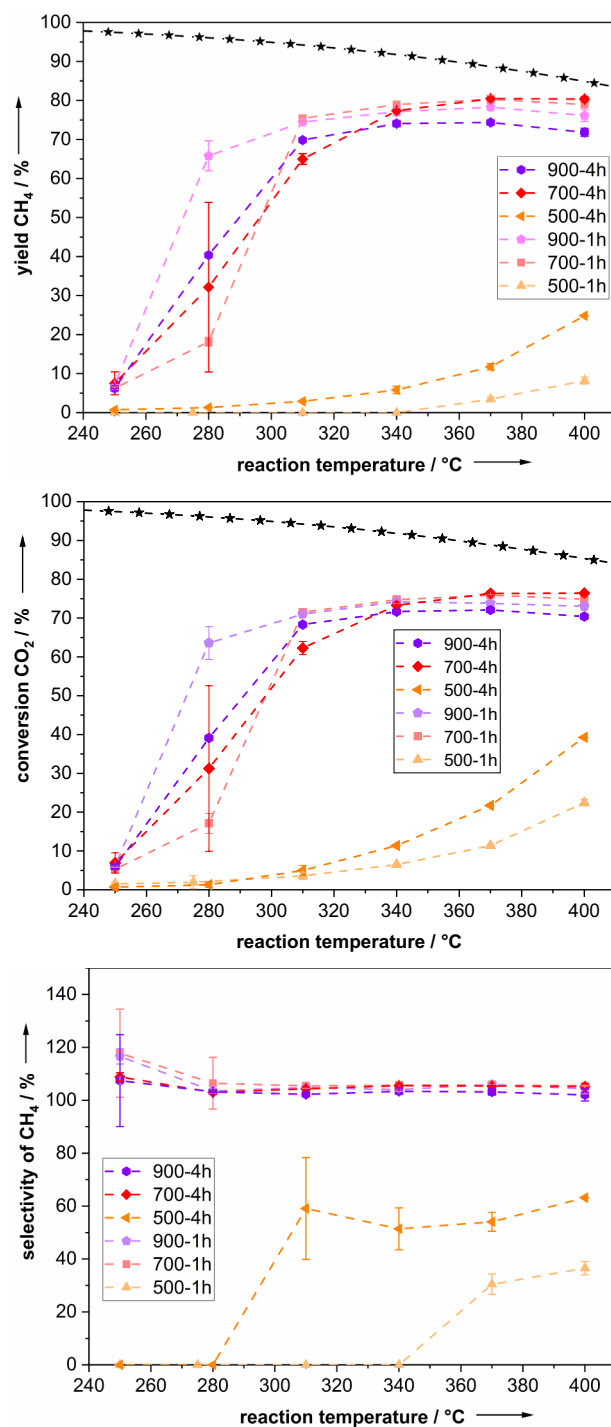
Fig. 5 Top: methane yield of catalysts from previously calcined precursors reduced at different conditions: orange triangle—reduction at 500 °C, red square—reduction at 700 °C, violet circle—reduction at 900 °C and reduced for different periods of time; black stars—thermodynamic equilibrium. Middle: CO₂ conversion, Bottom: selectivities corresponding to the measurements in Fig. 5 top

For the second series of measurements, in which the dried catalysts were calcined prior to the reduction, the catalytic activity and the selectivity are shown in Fig. 5. The catalysts previously calcined display in cases of high temperature reduction a similar behavior, qualitatively and quantitatively, as the directly reduced ones. For samples reduced at 700 and 900 °C, a constant methane yield of 80% is achieved at temperatures above 340 °C. In contrast,

the samples reduced at 500 °C display below 340 °C only yields less than 10% and just the samples reduced for 4 h exceed this value above this temperature. The selectivities of the calcined samples are similar to those of the directly reduced samples. If the reduction was carried out at 700 °C or 900 °C, a selectivity of approximately 100% is obtained over the entire temperature range (see Fig. 5, bottom) whereas samples reduced at 500 °C display only rather poor selectivity values of about 60% in the best cases.

Comparing the yields between the directly reduced and the samples calcined prior to reduction, there are significant differences. The reduction at 500 °C results only in low methane yields for temperatures up to 340 °C for both preparation routes, but above 340 °C the directly reduced catalyst achieves a much higher methane yield with values up to 65% compared to the calcined ones with values just up to 30%. If the reduction temperature is 700 °C applied for a reduction period of 4 h, the difference between the two preparation routes becomes most apparent because the directly reduced catalyst reveals at a temperature as low as 250 °C a performance in respect to yield and selectivity that is only matched by the calcined catalysts at a temperature at least 100 °C higher.

Regarding the performance of all directly reduced catalysts, it can be stated that they all together achieve equivalent or higher methane yields and CO$_2$ conversions than their calcined counterparts over the whole investigated temperature range. In contrast, the calcined samples only reach yields which are approximately equivalent to those of the directly reduced catalysts above 310 °C. It is noteworthy regarding these systems that there is no clear correlation between the BET surface area values and the respective catalytic activity. Although the samples directly reduced at 500 °C have the largest specific surface, they display a low degree of activity. This can be explained regarding the corresponding XRD measurements. In the XRD pattern in Fig. 2 the reflection for metallic nickel is essentially missing, which indicates that there is probably not enough metallic nickel to generate high catalytic activity. In contrast, strong nickel reflections are present in the case of direct reductions at 700 and 900 °C. But also for these systems, the relationship between surface area and catalytic activity is not following a clear trend if the variation in regard to surface area and reduction duration is considered. The activity of these samples differs strongly in the low temperature range (app. from 250

to 340 °C) and reaches similar yield values at high temperatures. However, in the low temperature region there is a significant difference and while the samples directly reduced at 900 °C do not show a significant performance difference in regard to the reduction duration, which could be seen in agreement with their similar BET surface area values, the sample reduced at 700 °C show such differences. While the 700 °C —4 h sample displays almost the same activity over the whole temperature range down to 250 °C, the activity of the 700 °C—1 h sample has continuously declined with the decrease of the reaction temperature displaying a yield of less than 10% at 250 °C, although both catalysts are comparably similar in respect to the measured surface area. The strong performance difference in respect to the temperature variation demonstrates that there must also be differences in the catalyst composition resulting from the preparation procedure that go beyond a mere difference in the number of active sites and that the proposed catalyst synthesis protocol leads to a very active catalyst.

A synthesis protocol of a very active catalyst without a separate calcination step has been reported before [26], but the group did not conduct a direct comparison between the preparation with and without such a step, so that observed high activity cannot be attributed to it, exclusively.

Conventional, non-hydrotalcite derived nickel catalysts show significant lower activities in CO$_2$ methanation than the here presented hydrotalcite derived ones. Garbarino et al. [32] investigated a commercially available Ni/Al$_2$O$_3$ catalyst and Guo et al. [33] impregnated nickel on aluminum and silicon oxide. In all three cases, the observed activities are below the activities of all in this study presented catalysts reduced at 700 or 900 °C. They only could reach comparable activities at reaction temperatures at about 400 °C, displaying an eminently lower activity increase with increasing reaction temperature. Of course, the comparison with literature data is often difficult, since the conditions in the catalytic studies usually differ slightly as a consequence of reactor design differences. However, in one of our previous publications [23], we report about the investigation of a non-hydrotalcite derived Ni/Al$_2$O$_3$ catalyst, tested at conditions comparable to the ones in this study. The activity of the catalyst showed a quantitatively and qualitatively behavior comparable to those discussed by Garbarino et al. and Guo et al. From this comparison, one can conclude that the hydrotalcite derived catalysts, especially if they are prepared by direct reduction, show a significant advantage in CO$_2$ methanation over those conventional types of catalyst.

3.3 TG-FTIR Coupling Experiments

The TG-FTIR measurements were carried out under H$_2$ atmosphere to track the reduction reaction. Figure 6 (top) shows the mass loss of the dried precursor upon heating.
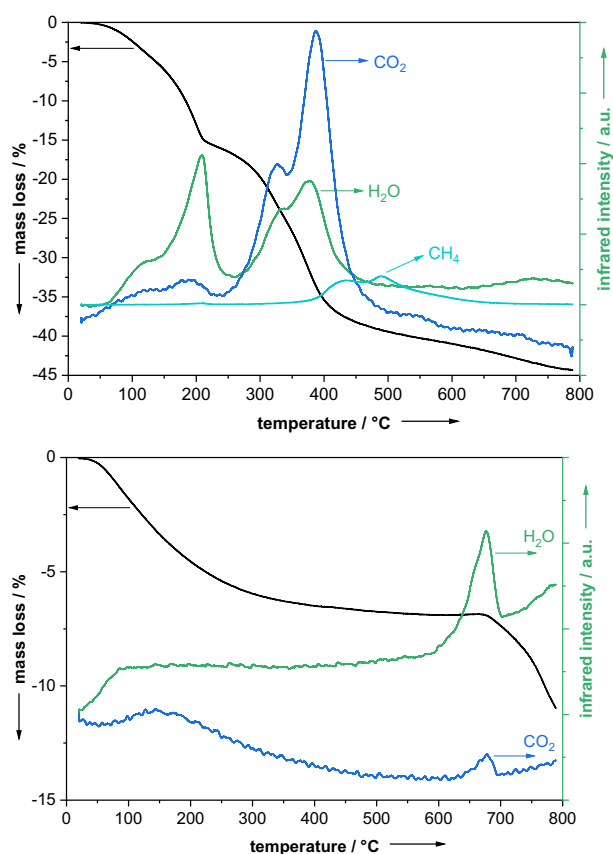
Fig. 6 TG-FTIR temperature programmed measurement of dried precursor (top) and previously calcined (bottom) material to track the progress of the reduction and the gaseous products emitted

Table 2 Degree of reduction and Ni:Mg ratio at surface determined by XPS measurements for directly reduced ('Direct') and previously calcined reduced ('Prev. calc.') samples for the given different reduction protocols (temperature—duration)

Reduction protocol	Degree of reduction		Ni:Mg ratio	
	Direct %	Prev. calc %	Direct	Prev. calc
500 °C—8 h	0	0	0.21	0.17
700 °C—1 h	14	3	0.14	0.15
700 °C—4 h	54	15	0.10	0.12
900 °C—1 h	65	63	0.08	0.06
900 °C—4 h	77	67	0.06	0.06

For the previously calcined material Fig. 6 (bottom) there are two steps of mass loss observable. The first one, starting nearly at room temperature, is accompanied only by weak FTIR signals of water and carbon dioxide. This mass loss originates from re-calcination of the material. As reported in literature [35] calcinated hydrotalcites tend to re-adsorb water und carbon dioxide from air. These adsorbed species are released during the first step of the shown TG curve. The second mass loss event starts at about 650 °C and is accompanied by a small FTIR signal of carbon dioxide and a larger signal of water. The signals derive mainly from an additional calcination step, which is completed at about 700 °C. At higher temperatures than that, the mass loss continues and the water signal stays detectable all the way to the maximum temperature of 800 °C presumably because of the subsequent reduction process of the precursor.

A comparison of these two measurements of the reduction process clearly shows that the required reduction temperature is significantly larger if the catalysts was previously calcined than if this was not the case. Therefore, it seems obvious that omitting the calcination step can lead to better reduced catalysts.

3.4 XPS Measurements

Table 2 summarizes the results of the XPS measurements. The degree of reduction in Table 2 was calculated from the ratio of the elemental nickel to the total nickel content on the sample surface. For the samples reduced at 500 °C, no elemental nickel was found, so the reduction degree is 0%. For the other samples there is a clear trend visible. The degree of reduction increases with increasing reduction temperature and duration. For all reduction protocols, the directly reduced sample shows a higher degree of reduction than the previously calcined samples, especially visible for the samples reduced at 700 °C. This observation fits well to the results of the TG-FTIR measurements.

The Ni:Mg ratios at the catalyst surfaces were also determined by XPS. They show a trend correlated to the reduction

The mass loss occurs over the entire temperature range in several phases. The first phase up to 200 °C is characterized by interlaminar water loss [34]. In the second phase up to 400 °C, water and CO_2 are released, which constitutes the actual calcination step [34].

Methane is formed between 400 and 500 °C, which is an indication that a part of the CO_2 released by the precursor while heating up is hydrogenated. The intensity of the methane signal increases up to 500 °C. The higher the temperature, the more methane is formed. Since in the given catalyst system metallic nickel appears to be necessary for this reaction, a part of the present nickel species must have been reduced even at these low temperatures.

From approximately 650 °C onward to higher temperatures, the water signal increases slightly again. The maximum of this water signal at a heating rate of (5 K/min) is approximately at 700 °C and the process appears to continue up to the final temperature of the experiment at 800 °C and beyond, although the transport kinetics for the gas to be released from the powder sample may be responsible for a certain delay of the corresponding signal.

protocols applied. The ratios are decreasing with increasing reduction temperature and duration which means that the nickel content at the surface decreases with the increase of these to parameters, since the diffusion of magnesium oxide appears to be unlikely. However, the Ni:Mg ratios stay almost the same if directly reduced and the previously calcined samples are compared.

Regarding the joint effect on the presence of elemental nickel on the surface of reduction degree and amount of nickel on the catalyst surface, ones sees that an increase of temperature and duration in the reduction process leads to opposing effects. In addition, the BET surface area also decreases (see Table 1) with these reduction parameters. Consequently, there will be an optimum in respect to the applied reduction temperature and the duration of the reduction process. At the same time, the directly reduced samples show higher reduction degrees and higher BET surface areas values than the previously calcined ones while the nickel content at surface stays approximately the same. From these observations, the results of the catalytic measurements can be explained. The directly reduced samples showed a higher activity than the previously calcined ones because of their higher amount of reduced nickel on surface. Comparing only the directly reduced samples with each other, the catalyst reduced at 700 °C for 4 h seems to be close to the optimum in respect to reduction temperature and duration resulting in the best compromise between high degree of reduction, high BET surface area, and a high amount of nickel on the catalyst surface. Altogether, this compromise leads to the highest amount of reduced nickel exposed to the reactants and thus to the most active catalyst.

4 Conclusions

It has been shown that omitting the calcination process that is part of the standard catalysts preparation from precursor materials obtained by precipitation from metal salt solutions can be advantageous to achieve very high catalytic activity in the case of nickel-hydrotalcite derived catalysts. For these catalysts, the activity was optimized by varying the reduction temperature and duration to the extent that consistently high methane yields have been achieved even at a reaction temperature that is approximately 100 °C lower than for the same yields by similar catalysts. For the presented nickel hydrotalcite derived catalyst, the highest catalytic activity was gained so far, if the reduction in a stream of gas composed of 5 vol% hydrogen in argon is carried out at a temperature of 700 °C for 4 h. This result is in accordance with the ones obtained by temperature dependent TG-FTIR measurements of the precursor material, which demonstrate a local maximum of water production in the high temperature region at 650 °C. Although the reduction occurs predominantly at these high temperatures, the formation of

methane at 400 °C indicates the presence of catalytically active centers and thus that the formation of metallic nickel from the precursor material must already occur at such a low temperature. However, a temperature above 650 °C is needed to generate a highly active catalyst.

It is clear that a high temperature treatment especially with reduced catalytic material can lower the catalytic activity by sintering the metallic particles and thus reduce the surface area of the catalytic active component and its accessibility for the reactants as shown by XPS measurements. In addition, the formation of spinels was observed along with the reduced catalytic activity for nickel-hydrotalcite systems if the reduction was carried out at 900 °C. While increased reduction temperatures improve the reduction degree, the BET surface area and the nickel content at surface on the other hand are decreasing. Therefore, there will be an optimal reduction temperature and duration for generating the most active catalysts. For the investigated catalysts in this study, this optimum appears to be close to a reduction temperature of 700 °C and a duration of 4 h.

The presented investigation also demonstrates that not only the high temperature treatment during reduction but also during calcination, if a separate calcination step is applied, can be harmful and it can be beneficial as in the case of the nickel-hydrotalcites to omit the calcination step completely. By omitting the calcination step an increased reduction degree and increased BET surface area values can be reached, resulting in a more active catalyst.

In the case of the nickel-hydrotalcites, a comparison of the synthesis routes, i.e. with and without a calcination step prior to reduction, reveals a dramatic effect in the catalyst performance especially at temperatures below 310 °C, where the same reaction rate is found almost at a temperature 100 centigrade lower as for the calcined counterparts.

Declarations

References

1. Barbarossa V, Vanga G, Viscardi R et al (2014) CO2 as carbon source for fuel synthesis. Energy Procedia 45:1325–1329. https://doi.org/10.1016/j.egypro.2014.01.138

2. Wang X, Zhen T, Yu C (2016) Application of Ni–Al-hydrotalcite-derived catalyst modified with Fe or Mg in CO2 methanation. Appl Petrochem Res 6:217–223. https://doi.org/10.1007/s13203-016-0154-1

3. Wierzbicki D, Debek R, Motak M et al (2016) Novel Ni-La-hydrotalcite derived catalysts for CO2 methanation. Catal Commun 83:5–8. https://doi.org/10.1016/j.catcom.2016.04.021

4. Ghaib K, Nitz K, Ben-Fares F-Z (2016) Chemical methanation of CO 2: a review. ChemBioEng Rev 3:266–275. https://doi.org/10.1002/cben.201600022

5. Stangeland K, Kalai D, Li H et al (2017) CO2 methanation: the effect of catalysts and reaction conditions. Energy Procedia 105:2022–2027. https://doi.org/10.1016/j.egypro.2017.03.577

6. Abate S, Barbera K, Giglio E et al (2016) Synthesis, characterization, and activity pattern of Ni–Al hydrotalcite catalysts in CO2 methanation. Ind Eng Chem Res 55:8299–8308. https://doi.org/10.1021/acs.iecr.6b01581

7. Mette K, Kühl S, Düdder H et al (2014) Stable performance of ni catalysts in the dry reforming of methane at high temperatures for the efficient conversion of CO2 into syngas. ChemCatChem 6:100–104. https://doi.org/10.1002/cctc.201300699

8. Yao L, Wang Y, Shi J et al (2017) The influence of reduction temperature on the performance of ZrOx/Ni–MnOx/SiO2 catalyst for low-temperature CO2 reforming of methane. Catal Today 281:259–267. https://doi.org/10.1016/j.cattod.2016.05.031

9. Valle B, Aramburu B, Remiro A et al (2014) Effect of calcination/reduction conditions of Ni/La2O3–αAl2O3 catalyst on its activity and stability for hydrogen production by steam reforming of raw bio-oil/ethanol. Appl Catal B 147:402–410. https://doi.org/10.1016/j.apcatb.2013.09.022

10. Chang F-W, Tsay M-T, Kuo M-S (2002) Effect of thermal treatments on catalyst reducibility and activity in nickel supported on RHA–Al2O3 systems. Thermochim Acta 386:161–172. https://doi.org/10.1016/S0040-6031(01)00771-7

11. Usman M, Wan Daud WMA (2016) An investigation on the influence of catalyst composition, calcination and reduction temperatures on Ni/MgO catalyst for dry reforming of methane. RSC Adv 6:91603–91616. https://doi.org/10.1039/C6RA15256B

12. Behrens M (2015) Coprecipitation: an excellent tool for the synthesis of supported metal catalysts—from the understanding of the well known recipes to new materials. Catal Today 246:46–54. https://doi.org/10.1016/j.cattod.2014.07.050

13. Bi X, Zhang H, Dou L (2014) Layered double hydroxide-based nanocarriers for drug delivery. Pharmaceutics 6:298–332. https://doi.org/10.3390/pharmaceutics6020298

14. Dębek R, Radlik M, Motak M et al (2015) Ni-containing Ce-promoted hydrotalcite derived materials as catalysts for methane reforming with carbon dioxide at low temperature—on the effect of basicity. Catal Today 257:59–65. https://doi.org/10.1016/j.cattod.2015.03.017

15. Frontera P, Macario A, Ferraro M et al (2017) Supported catalysts for CO2 methanation: a review. Catalysts 7:59. https://doi.org/10.3390/catal7020059

16. He L, Lin Q, Liu Y et al (2014) Unique catalysis of Ni-Al hydrotalcite derived catalyst in CO2 methanation: cooperative effect between Ni nanoparticles and a basic support. J Energy Chem 23:587–592. https://doi.org/10.1016/S2095-4956(14)60144-3

17. Vaccari A (1998) Preparation and catalytic properties of cationic and anionic clays. Catal Today 41:53–71. https://doi.org/10.1016/s0920-5861(98)00038-8

18. Gabrovska M, Edreva-Kardjieva R, Crişan D et al (2012) Ni–Al layered double hydroxides as catalyst precursors for CO2 removal by methanation. Reac Kinet Mech Cat 105:79–99. https://doi.org/10.1007/s11144-011-0378-0

19. Bette N, Thielemann J, Schreiner M et al (2016) Methanation of CO2 over a (Mg, Al)O x supported nickel catalyst derived from a (Ni, Mg, Al)-hydrotalcite-like precursor. ChemCatChem 8:2903–2906. https://doi.org/10.1002/cctc.201600469

20. Wierzbicki D, Baran R, Dębek R et al (2017) The influence of nickel content on the performance of hydrotalcite-derived catalysts in CO2 methanation reaction. Int J Hydrog Energy 42:23548–23555. https://doi.org/10.1016/j.ijhydene.2017.02.148

21. Guo X, Peng Z, Hu M et al (2018) Highly active Ni-based catalyst derived from double hydroxides Precursor for low temperature CO2 methanation. Ind Eng Chem Res 57:9102–9111. https://doi.org/10.1021/acs.iecr.8b01619

22. Wierzbicki D, Motak M, Grzybek T et al (2018) The influence of lanthanum incorporation method on the performance of nickel-containing hydrotalcite-derived catalysts in CO2 methanation reaction. Catal Today 307:205–211. https://doi.org/10.1016/j.cattod.2017.04.020

23. Völs P, Hilbert S, Störr B et al (2021) Methanation of CO2 and CO by (Ni, Mg, Al)-hydrotalcite-derived and related catalysts with varied magnesium and aluminum oxide contents. Ind Eng Chem Res 60:5114–5123. https://doi.org/10.1021/acs.iecr.1c00028

24. León M, Díaz E, Bennici S et al (2010) Adsorption of CO2 on hydrotalcite-derived mixed oxides: sorption mechanisms and consequences for adsorption irreversibility. Ind Eng Chem Res 49:3663–3671. https://doi.org/10.1021/ie902072a

25. Roelofs JCAA, van Bokhoven JA, van Dillen AJ et al (2002) The thermal decomposition of Mg-Al hydrotalcites: effects of interlayer anions and characteristics of the final structure. Chem Eur J 8:5571–5579. https://doi.org/10.1002/1521-3765(20021216)8:24%3c5571:AID-CHEM5571%3e3.0.CO;2-R

26. Guo X, Gao D, He H et al (2021) Promotion of CO2 methanation at low temperature over hydrotalcite-derived catalysts-effect of the tunable metal species and basicity. Int J Hydrog Energy 46:518–530. https://doi.org/10.1016/j.ijhydene.2020.09.193

27. Lima DdS, Dias YR, Perez-Lopez OW (2020) CO2 methanation over Ni–Al and Co–Al LDH-derived catalysts: the role of basicity. Sustain Energy Fuels 4:5747–5756. https://doi.org/10.1039/D0SE01059F

28. Marocco P, Morosanu EA, Giglio E et al (2018) CO2 methanation over Ni/Al hydrotalcite-derived catalyst: experimental characterization and kinetic study. Fuel 225:230–242. https://doi.org/10.1016/j.fuel.2018.03.137

29. Düdder H, Kähler K, Krause B et al (2014) The role of carbonaceous deposits in the activity and stability of Ni-based catalysts applied in the dry reforming of methane. Catal Sci Technol 4:3317–3328. https://doi.org/10.1039/C4CY00409D

30. Haycock DE, Kasrai M, Nicholls CJ et al (1978) The electronic structure of magnesium hydroxide (brucite) using X-ray emission, X-ray photoelectron, and auger spectroscopy. J Chem Soc. https://doi.org/10.1039/dt9780001791

31. Garcia L, Salvador ML, Bilbao R et al (1998) Influence of calcination and reduction conditions on the catalyst performance in the pyrolysis process of biomass. Energy Fuels 12:139–143. https://doi.org/10.1021/EF970097J

32. Garbarino G, Bellotti D, Riani P et al (2015) Methanation of carbon dioxide on Ru/Al2O3 and Ni/Al2O3 catalysts at atmospheric pressure: catalysts activation, behaviour and stability. Int J Hydrog Energy 40:9171–9182. https://doi.org/10.1016/j.ijhydene.2015.05.059

33. Guo X, Traitangwong A, Hu M et al (2018) Carbon dioxide methanation over nickel-based catalysts supported on various

mesoporous material. Energy Fuels 32:3681–3689. https://doi.org/10.1021/acs.energyfuels.7b03826

34. Romero A, Jobbágy M, Laborde M et al (2010) Ni(II)–Mg(II)–Al(III) catalysts for hydrogen production from ethanol steam reforming: influence of the activation treatments. Catal Today 149:407–412. https://doi.org/10.1016/j.cattod.2009.05.026

35. Cavani F, Trifirò F, Vaccari A (1991) Hydrotalcite-type anionic clays: preparation, properties and applications. Catal Today 11:173–301. https://doi.org/10.1016/0920-5861(91)80068-K

Authors and Affiliations

Alexandra Müller[1] · Pit Völs[1] · Bianca Störr[1] · Florian Mertens[1]

✉ Florian Mertens
florian.mertens@chemie.tu-freiberg.de

[1] Department of Physical Chemistry, TU Bergakademie Freiberg, Leipziger Straße 29, 09599 Freiberg, Germany